Available online at www.sciencedirect.com
ScienceDirect
Comput. Methods Appl. Mech. Engrg. 393 (2022) 114792
Computer methods in applied mechanics and engineering
www.elsevier.com/locate/cma

The finite cell method with least squares stabilized Nitsche boundary conditions

Karl Larsson[a,*], Stefan Kollmannsberger[b], Ernst Rank[b], Mats G. Larson[a]

[a] *Mathematics and Mathematical Statistics, Umeå University, Sweden*
[b] *Chair of Computational Modeling and Simulation, TUM, Germany*

Received 27 October 2021; received in revised form 18 February 2022; accepted 19 February 2022
Available online xxxx

Abstract

We apply the recently developed least squares stabilized symmetric Nitsche method for enforcement of Dirichlet boundary conditions to the finite cell method. The least squares stabilized Nitsche method in combination with finite cell stabilization leads to a symmetric positive definite stiffness matrix and relies only on elementwise stabilization, which does not lead to additional fill in. We prove a priori error estimates and bounds on the condition numbers.
© 2022 The Author(s). Published by Elsevier B.V. This is an open access article under the CC BY license (http://creativecommons.org/licenses/by/4.0/).

Keywords: Finite cell method; Dirichlet conditions; Nitsche's method; A priori error estimates

1. Introduction

Unfitted finite element methods allow for the geometry of the problem domain to cut through the underlying computational mesh in an arbitrary manner and avoid the use of standard meshing tools. Over recent years several methods that deal with the challenges of unfitted FEM in slightly different ways have been proposed, see for instance [1–5].

In this contribution we provide an analysis for an unfitted FEM, the finite cell method [1], when combined with an improved technique for weakly imposing Dirichlet boundary conditions. Specifically, we address the following two central issues that naturally arise when developing unfitted FEMs:

1. Enforcing Dirichlet boundary conditions. In contrast to classical FEMs the degrees of freedom in unfitted FEMs are no longer nodal values coinciding with the boundary. A very elegant solution for dealing with this issue is weak enforcement via Nitsche's method, first introduced in 1971 by Nitsche in his seminal work [6]. Weak enforcement of Dirichlet boundary conditions does seem to be a perfect match with unfitted methods and the elegance of this particular method shows in optimal order error bounds using only a h^{-1} scaling of the penalty parameter. However,

* Corresponding author.
E-mail addresses: karl.larsson@umu.se (K. Larsson), stefan.kollmannsberger@tum.de (S. Kollmannsberger), ernst.rank@tum.de (E. Rank), mats.larson@umu.se (M.G. Larson).

https://doi.org/10.1016/j.cma.2022.114792
0045-7825/© 2022 The Author(s). Published by Elsevier B.V. This is an open access article under the CC BY license (http://creativecommons.org/licenses/by/4.0/).

the stability analysis in [6] utilizes an inverse inequality that does not hold by default for unfitted finite elements, whereby additional stabilization is required for a complete analysis.

2. Ensuring stability and accuracy. While there are clear modeling benefits of an unfitted FEM approach, a drawback is that there may exist basis functions in our computational grid whose support has a negligible intersection with the domain. This takes its expression in the form of two stability issues that are related but not the same:

- *Stability of formulation.* For elliptic PDE, as we consider in this contribution, this means a guaranteed coercive method. If the method is not coercive, we cannot be sure we are actually solving the correct problem, even if we may solve the resulting linear system of equations without any hassle.
- *Stability of linear system of equations.* This means there exists an upper bound on the condition number for the stiffness matrix.

To mitigate these stability issues several approaches have been proposed in literature, for instance; ghost penalty stabilization [3,7]; element merging [8]; removal of problematic basis functions [9]; and finite cell stabilization [10,11].

The finite cell method. As a framework for unfitted FEMs, addressing problems of discretization, quadrature, and stability, the finite cell method (FCM) was originally introduced in [1] and has since successfully been applied to a wide variety of applications, for instance in solid mechanics [5,12], structural analysis [13,14], and fluid–structure interaction [15]. In this work, the focus is on the stability issues and the mathematical analysis of the method. The principal stabilization technique in FCM is based on adding a small virtual stiffness in parts of elements that are exterior to the domain, and this we refer to as *finite cell stabilization*. In the case of Neumann conditions, an analysis of finite cell stabilization was provided in [10], while we in the present contribution provide an analysis in the case of weakly enforced Dirichlet conditions.

Summary of contribution. In this paper we develop a new symmetric finite cell method which utilizes the recently developed least-squares stabilized Nitsche formulation (LS-Nitsche) [16] for weakly enforcing the Dirichlet boundary conditions. We work in a higher regularity space $V = H^2(\Omega)$ setting and we therefore consider C^1 splines constructed on a background grid as our approximation space V_h. The following key considerations are taken into account:

- *Stability of formulation.* The use of LS-Nitsche [16] appends the standard Nitsche formulation by certain least squares terms in the vicinity of the boundary as well as control over the tangent gradient along the boundary, yielding a formulation which is stable not only on the discrete space V_h but on $V = H^2(\Omega)$. Effectively, this means the method is coercive regardless of the cut situation even without any finite cell stabilization.
- *Stability of linear system of equations.* Since coercivity is ensured via LS-Nitsche, the focus of the finite cell stabilization, i.e. the virtual stiffness added inside cut elements outside of the domain, is to guarantee stability of the linear system of equations. If finite cell stabilization is not included, the norm in which coercivity is proven will only be a seminorm on V_h since V_h in certain cut situations may include functions whose support has an arbitrarily small intersection with the domain. This, in effect, gives a stiffness matrix which is only guaranteed to be symmetric positive semidefinite, while including finite cell stabilization will move the stiffness matrix to be symmetric positive definite (SPD). We include an error analysis, that identifies the suitable choice of the finite cell stabilization parameter. Note that thanks to LS-Nitsche we already have coercivity and only very weak virtual stiffness needs to be added to ensure that the stiffness matrix is SPD. Our results complements [10] where Neumann conditions are analyzed.
- *Implementation and use.* In the method, all terms are assembled element-wise making for a very straightforward implementation. For this to hold the added smoothness of the spline space is utilized in the derivations of the least-squares terms. A feature of LS-Nitsche that simplifies the use of the method is that the choice of penalty parameter does not depend on the cut situation. Furthermore, a modest value for the penalty parameter may be chosen which allows complex geometries even at the element level, without locking [16].

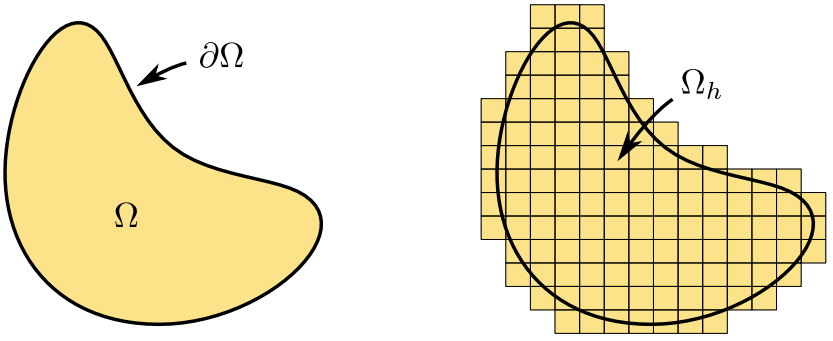

(a) Problem domain **(b)** Domain of active elements

Fig. 1. (a) The domain Ω of the model problem. (b) The domain of all active elements Ω_h, i.e. the union of all elements with a non-empty intersection with the domain Ω.

Outline. The paper is organized as follows. In Section 2 we introduce our method; an unfitted finite element method featuring least-squares stabilized Nitsche boundary conditions and finite cell stabilization. In Section 3 we prove stability and error estimates in the energy and L^2 norms. In Section 4 we derive a bound on the condition number. In Section 5 we present illustrating numerical examples. Finally, in Section 6 we present our conclusions.

2. The finite cell method with LS-Nitsche

2.1. Model problem

Let Ω be a domain in $\mathbb{R}^d$ with smooth boundary $\partial\Omega$, such as illustrated in Fig. 1(a), and consider the problem: find $u : \Omega \to \mathbb{R}$ such that

$$-\Delta u = f \qquad \text{in } \Omega \tag{2.1}$$

$$u = g \qquad \text{on } \partial\Omega \tag{2.2}$$

For sufficiently regular data there exists a unique solution to this problem and we will be interested in higher order methods and therefore we will always assume that the solution satisfies the regularity estimate

$$\|u\|_{H^{s+2}(\Omega)} \lesssim \|f\|_{H^s(\Omega)} + \|g\|_{H^{s-1/2}(\partial\Omega)} \tag{2.3}$$

for some $s \geq 0$. Here and below $a \lesssim b$ means that there is a positive constant C independent of the mesh parameter h and the cut situation such that $a \leq Cb$.

2.2. The B-spline spaces

Definitions.

- Let $\widetilde{\mathcal{T}}_h$, $h \in (0, h_0]$, be a family of uniform tensor product meshes in $\mathbb{R}^d$ with mesh parameter h.
- Let $\widetilde{V}_h = C^{p-1}Q^p(\mathbb{R}^d)$ be the space of C^{p-1} tensor product B-splines of order p defined on $\widetilde{\mathcal{T}}_h$. Such functions are easily generated using the Cox–de Boor recursion formula. Let $\widetilde{B} = \{\varphi_i\}_{i\in\widetilde{I}}$ be the standard basis in $\widetilde{V}_h$, where $\widetilde{I}$ is an index set.
- Let $B = \{\varphi \in \widetilde{B} : \text{supp}(\varphi) \cap \Omega \neq \emptyset\}$ be the set of basis functions with support that intersects Ω. Let $V_h = \text{span}\{B\}$, $\mathcal{T}_h = \{T \in \widetilde{\mathcal{T}}_h : T \cap \Omega \neq \emptyset\}$, and $\Omega_h = \cup_{T\in\mathcal{T}_h} T$. An illustration of the basis functions in one spatial dimension is given in Fig. 2 and Ω_h is illustrated in Fig. 1(b).
- We will only consider $p \geq 2$ corresponding to at least C^1 splines. We then have $V_h|_\Omega \subset V = H^2(\Omega)$.

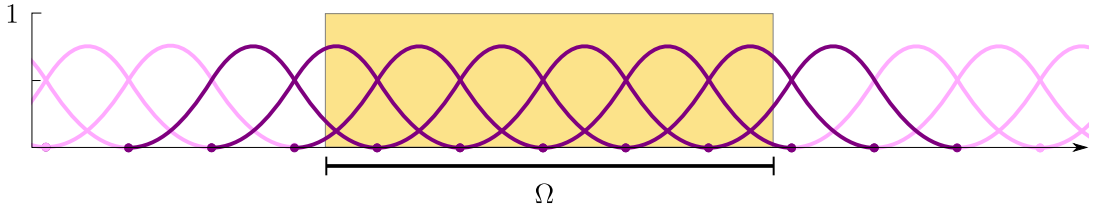

Fig. 2. $C^1Q^2(\mathbb{R})$ B-spline basis functions in one dimension. The set B of basis functions with non-empty support in Ω is indicated in deep purple. Note that basis functions crossing the boundary of Ω are defined analogously to interior basis functions.

2.3. The method

Method. Find $u_{h,\alpha} \in V_h$ such that

$$A_{h,\alpha}(u_{h,\alpha}, v) = L_h(v) \qquad \forall v \in V_h \tag{2.4}$$

The forms are defined as follows:

$$A_{h,\alpha}(v, w) = a_h(v, w) + \overbrace{\alpha(\nabla v, \nabla w)_{\Omega_h \setminus \Omega}}^{\text{Finite cell stabilization}} \tag{2.5}$$

$$\underbrace{-(\nabla_n v, w)_{\partial\Omega} - (v, \nabla_n w)_{\partial\Omega} + \beta b_h(v, w)}_{\text{Nitsche BC terms}} \tag{2.6}$$

$$a_h(v, w) = (\nabla v, \nabla w)_\Omega + \underbrace{\tau h^2 (\Delta v, \Delta w)_{\mathcal{T}_{h,\partial\Omega} \cap \Omega}}_{\text{New LS interior term}} \tag{2.7}$$

$$b_h(v, w) = (2 + \tau^{-1}) h^{-1} (v, w)_{\partial\Omega} + \underbrace{2h(\nabla_T v, \nabla_T w)_{\partial\Omega}}_{\text{New LS boundary term}} \tag{2.8}$$

$$L_h(v) = (f, v)_\Omega \underbrace{-\tau h^2 (f, \Delta v)_{\mathcal{T}_{h,\partial\Omega} \cap \Omega}}_{\text{New LS interior term}} \underbrace{-(g, \nabla_n v)_{\partial\Omega} + \beta b_h(g, v)}_{\text{Nitsche BC terms}} \tag{2.9}$$

Parameters. The included parameters are:

- $\alpha \geq 0$ is the finite cell stabilization parameter, which we will define as $\alpha \sim h^{2p-1}$ to obtain a scheme with optimal order convergence. This stabilization provides a small virtual stiffness in exterior parts of cut elements which, for the present method, is crucial for guaranteeing stability of the linear system of equations.
- $\beta > 0$ is a penalty parameter of moderate size, for instance $\beta = 5$ is sufficient, see [16].
- $\tau > 0$ can be chosen in order to optimize accuracy, where typical values are in the range 0.01–1, see [16]. The effective parameter in front of the standard Nitsche penalty term $h^{-1}(v, w)_{\partial\Omega}$ is $\beta(2 + \tau^{-1})$ and thus τ trades control between the interior least squares term $h^2(\Delta v, \Delta w)_{\mathcal{T}_{h,\partial\Omega} \cap \Omega}$ and the standard Nitsche penalty term.

Notation. We employed the following notation:

- $\nabla_n = n \cdot \nabla$ is the normal derivative on the boundary $\partial\Omega$ where n is the exterior unit normal to $\partial\Omega$.
- $\nabla_T = P\nabla$ is the so-called tangent gradient on $\partial\Omega$ where $P = (I - n \otimes n)$ is the projection onto the tangent plane of $\partial\Omega$.
- $\mathcal{T}_{h,\partial\Omega} \cap \Omega = \cup_{T \in \mathcal{T}_{h,\partial\Omega}} T \cap \Omega$ is the interior region of least squares stabilization, see Fig. 3, where the set $\mathcal{T}_{h,\partial\Omega} \subset \mathcal{T}_h$ is defined

$$\mathcal{T}_{h,\partial\Omega} = \mathcal{T}_h(U_h(\partial\Omega)) = \{T \in \mathcal{T}_h : T \cap U_h(\partial\Omega) \neq \emptyset\} \tag{2.10}$$

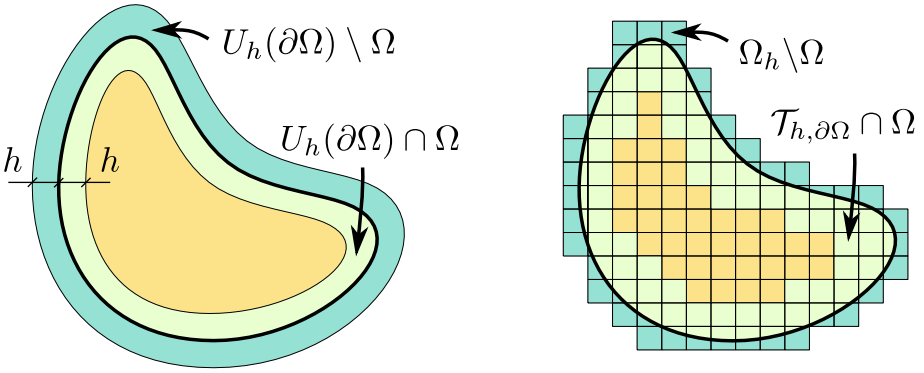

Fig. 3. Illustrations of geometrical regions used in the method and throughout the analysis. By construction $(U_h(\partial\Omega) \cap \Omega) \subseteq (\mathcal{T}_{h,\partial\Omega} \cap \Omega)$ and $(\Omega_h \setminus \Omega) \subseteq (U_h(\partial\Omega) \setminus \Omega)$.

and $U_h(\partial\Omega)$ is the tubular neighborhood

$$U_h(\partial\Omega) = \bigcup_{x\in\partial\Omega} B_h(x) \tag{2.11}$$

with $B_h(x)$ the open ball with center x and radius h. Integrals over $\mathcal{T}_{h,\partial\Omega} \cap \Omega$ are evaluated elementwise such that

$$(v, w)_{\mathcal{T}_{h,\partial\Omega}\cap\Omega} = \sum_{T\in\mathcal{T}_{h,\partial\Omega}} (v, w)_{T\cap\Omega} \tag{2.12}$$

Remark 2.1. In practice, $\mathcal{T}_{h,\partial\Omega}$ may be taken as the set of all elements that intersect the Dirichlet boundary $\partial\Omega$ and their neighbors, i.e., $\mathcal{T}_{h,\partial\Omega} = \mathcal{N}_h(\mathcal{T}_h(\partial\Omega))$.

Commentary on LS terms. The added least-squares terms, $h^2(\Delta v, \Delta w)_{\mathcal{T}_{h,\partial\Omega}\cap\Omega}$ and $h(\nabla_T v, \nabla_T w)_{\partial\Omega}$, provide additional control on the elements in the vicinity of the boundary and along the boundary. The additional control along the boundary may be interpreted as weak enforcement of Dirichlet boundary conditions in $H^{1/2}(\partial\Omega)$, the trace space of $H^1(\Omega)$, and we note that

$$h^{-1}\|v\|^2_{\partial\Omega} + h\|\nabla_T v\|^2_{\partial\Omega} \tag{2.13}$$

is a discrete version of $\|v\|^2_{H^{1/2}(\partial\Omega)}$, which is more precise compared to the standard Nitsche method due to the presence of the second term. In the case when we do not have any cut elements we may employ an inverse inequality to conclude that

$$h^{-1}\|v\|^2_{\partial\Omega} + h\|\nabla_T v\|^2_{\partial\Omega} \sim h^{-1}\|v\|^2_{\partial\Omega} \tag{2.14}$$

and we recover the standard Nitsche penalty term. This is however not possible in the cut case where the additional term plays a key role. Furthermore, for $w \in H^1(\Omega)$ we have the standard estimate

$$|(\nabla_n v, w)_{\partial\Omega}| \leq (\|\nabla v\|^2_\Omega + \|\Delta v\|^2_\Omega)^{1/2}\|w\|_{H^1(\Omega)} \tag{2.15}$$

and thus for the left hand side to be well posed we need control of $\|\Delta v\|_\Omega$ in addition to $\|\nabla v\|_\Omega$. We note that $h^2(\Delta v, \Delta w)_{\mathcal{T}_{h,\partial\Omega}\cap\Omega}$ and $h(\nabla_T v, \nabla_T w)_{\partial\Omega}$ provides such control close to the boundary, which turns out to be enough.

Finally, if we do not have cut elements an inverse inequality gives

$$h^2\|\Delta v\|_{\Omega}^2 \lesssim \|\nabla v\|_{\Omega}^2 \tag{2.16}$$

and thus in that case $h^2\|\Delta v\|_{\Omega}^2$ is dominated by $\|\nabla v\|_{\Omega}^2$, which is already present in the standard variational form.

3. Analysis of the method

3.1. Extension outside the domain

Throughout the analysis we need to evaluate functions in $V = H^2(\Omega)$ not only within Ω but also a region exterior to Ω, specifically within $U_h(\partial\Omega) \setminus \Omega$, see Fig. 3. For this we use the following known result; there is an extension operator $E : W_q^k(\Omega) \to W_q^k(\mathbb{R}^d)$, $k \geq 0$ and $q \geq 1$, such that $(Ev)|_{\Omega} = v$ and

$$\|Ev\|_{W_q^k(\mathbb{R}^d)} \lesssim \|v\|_{W_q^k(\Omega)} \tag{3.1}$$

see [17]. In particular we use this extension on the exact solution u in our derivations below, where we let u on $U_h(\partial\Omega) \cup \Omega$ be defined by u on Ω and by the extension Eu on $U_h(\partial\Omega) \setminus \Omega$.

3.2. Consistency

Galerkin orthogonality. With $u \in V = H^2(\Omega)$ the solution to (2.1)–(2.2) and $u_{h,\alpha} \in V_h$ the solution to (2.4) it holds

$$A_{h,\alpha}(u - u_{h,\alpha}, v) - \alpha(\nabla u, \nabla v)_{\Omega_h \setminus \Omega} = 0 \qquad \forall v \in V_h \tag{3.2}$$

where the second term on the right hand side accounts for the inconsistent finite cell stabilization.

Proof. We first recall that for $\alpha = 0$ the method is consistent, i.e. the exact solution u to (2.1)–(2.2) satisfies

$$A_{h,0}(u, v) = L_h(v) \qquad \forall v \in V_h \tag{3.3}$$

since the standard Nitsche method with $\gamma = 0$ and $\tau = 0$ is consistent and the added least squares terms are residual terms:

$$\Delta u + f = 0 \quad \Longrightarrow \quad \tau h^2(\Delta u, \Delta v)_{\mathcal{T}_{h,\partial\Omega}\cap\Omega} = -\tau h^2(f, \Delta v)_{\mathcal{T}_{h,\partial\Omega}\cap\Omega} \tag{3.4}$$

$$u|_{\partial\Omega} = g \quad \Longrightarrow \quad 2h(\nabla_T u, \nabla_T v)_{\partial\Omega} = 2h(\nabla_T g, \nabla_T v)_{\partial\Omega} \tag{3.5}$$

Next note that for $v \in V_h$ we have

$$0 = L_h(v) - A_{h,\alpha}(u_{h,\alpha}, v) \tag{3.6}$$

$$= A_{h,0}(u, v) - A_{h,\alpha}(u_{h,\alpha}, v) \tag{3.7}$$

$$= \big(A_{h,\alpha}(u, v) - \alpha(\nabla u, \nabla v)_{\Omega_h \setminus \Omega}\big) - A_{h,\alpha}(u_{h,\alpha}, v) \tag{3.8}$$

$$= A_{h,\alpha}(u - u_{h,\alpha}, v) - \alpha(\nabla u, \nabla v)_{\Omega_h \setminus \Omega} \quad \blacksquare \tag{3.9}$$

3.3. Energy norm

Recall that $V = H^2(\Omega)$ and $V_h|_{\Omega} \subset V$, and define the following norms on V,

$$|||v|||_{h,\alpha}^2 = |||v|||_h^2 + \alpha\|\nabla v\|_{\Omega_h \setminus \Omega}^2 \tag{3.10}$$

$$|||v|||_h^2 = \|v\|_{a_h}^2 + \|v\|_{b_h}^2 \tag{3.11}$$

$$\|v\|_{a_h}^2 = a_h(v, v) = \|\nabla v\|_{\Omega}^2 + \tau h^2\|\Delta v\|_{\mathcal{T}_{h,\partial\Omega}\cap\Omega}^2 \tag{3.12}$$

$$\|v\|_{b_h}^2 = b_h(v, v) = (2 + \tau^{-1})h^{-1}\|v\|_{\partial\Omega}^2 + 2h\|\nabla_T v\|_{\partial\Omega}^2 \tag{3.13}$$

Remark 3.1. Since V_h may contain basis functions whose support has an arbitrarily small intersection with Ω the energy norm (3.11) is only guaranteed to be a semi-norm on V_h in the case $\alpha = 0$ while it is a norm on V_h if $\alpha > 0$. For this reason we will need the finite cell stabilization to guarantee stability of the linear system of equations, see Section 4.

3.4. Results on LS-Nitsche

Here we summarize the main results on the LS-Nitsche method [16], which is essentially our method (2.4) in the case $\alpha = 0$. The central estimate in the analysis presented in [16] is the following bound on the normal flux form, from which coercivity and continuity results are readily established, requiring only minor adaptations to cover the present method when $\alpha > 0$.

Continuity of normal flux form. The following estimate holds

$$\left|(\nabla_n v, w)_{\partial\Omega}\right| \lesssim \|v\|_{a_h}\|w\|_{b_h} \qquad v, w \in V \tag{3.14}$$

where the hidden constant is close to one for h sufficiently small.

Coercivity. For $\beta > 0$ sufficiently large the form $A_{h,\alpha}$ is coercive

$$|||v|||^2_{h,\alpha} \lesssim A_{h,\alpha}(v, v) \qquad v \in V \tag{3.15}$$

Continuity. The form $A_{h,\alpha}$ is continuous

$$A_{h,\alpha}(v, w) \lesssim |||v|||_{h,\alpha}|||w|||_{h,\alpha} \qquad v, w \in V \tag{3.16}$$

Remark 3.2 (*Coercivity*)**.** Note that the coercivity holds on the full space $V = H^2(\Omega)$ and not only on the discrete space V_h as is the case in the standard analysis of Nitsche's method. The reason is that the LS-Nitsche formulation circumvents the use of an inverse inequality in the proof of the coercivity estimate. Also note that β being sufficiently large for the LS-Nitsche method actually translates into a quite moderate number, for instance $\beta = 5$ is sufficient. This is derived based on the good knowledge of the constant in (3.14). We refer to [16] for details.

Remark 3.3 (*Adaptation of proofs*)**.** In [16] the coercivity and continuity is established for $\alpha = 0$ and it follows directly from the definition of $A_{h,\alpha}$ and the norm $|||\cdot|||_{h,\alpha}$ that these results also hold for $A_{h,\alpha}$. For instance,

$$|||v|||^2_{h,\alpha} = |||v|||^2_{h,0} + \alpha\|\nabla v\|^2_{\Omega_h\setminus\Omega} \lesssim A_{h,0}(v, v) + \alpha(\nabla v, \nabla v)_{\Omega_h\setminus\Omega} = A_{h,\alpha}(v, v) \tag{3.17}$$

3.5. Interpolation error estimates

Define the interpolant by

$$\pi_h : H^s(\Omega) \ni u \mapsto \Pi_h(Eu) \in V_h \tag{3.18}$$

where $\Pi_h : H^s(\Omega_h) \mapsto V_h$ is a spline space quasi-interpolant, see [18]. We have the standard a priori error estimate

$$\|v - \pi_h v\|_{H^m(T)} \lesssim h^{s-m}\|v\|_{H^s(\mathcal{N}_h(T))} \tag{3.19}$$

where $\mathcal{N}_h(T) = \cup_{\varphi\in B(T)}\text{supp}(\varphi)$ and $B(T) = \{\varphi \in B : T \subset \text{supp}(\varphi)\}$. We have the interpolation estimate

$$|||v - \pi_h v|||_{h,\alpha} \lesssim h^p\|v\|_{H^{p+1}(\Omega)} \tag{3.20}$$

for $0 \le m \le s \le p + 1$.

3.6. Error estimates

Theorem 3.1 (*Energy norm error estimate*). *For $u \in H^{p+1}(\Omega)$ the following error estimate holds*

$$|\!|\!| u - u_{h,\alpha} |\!|\!|_{h,\alpha} \lesssim h^p \|u\|_{H^{p+1}(\Omega)} + \alpha^{1/2} h^{1/2} \|u\|_{H^2(\Omega)} \tag{3.21}$$

and with

$$\alpha \lesssim h^{2p-1} \tag{3.22}$$

we obtain

$$|\!|\!| u - u_{h,\alpha} |\!|\!|_{h,\alpha} \lesssim h^p \|u\|_{H^{p+1}(\Omega)} \tag{3.23}$$

Proof. We first have

$$|\!|\!| u - u_{h,\alpha} |\!|\!|_{h,\alpha} \lesssim |\!|\!| u - \pi_h u |\!|\!|_{h,\alpha} + |\!|\!| \pi_h u - u_{h,\alpha} |\!|\!|_{h,\alpha} \tag{3.24}$$

$$\lesssim h^p \|u\|_{H^{p+1}(\Omega)} + |\!|\!| \pi_h u - u_{h,\alpha} |\!|\!|_{h,\alpha} \tag{3.25}$$

where we used the interpolation estimate (3.20). In order to estimate the second term we start by using coercivity

$$|\!|\!| \pi_h u - u_{h,\alpha} |\!|\!|_{h,\alpha} \lesssim \sup_{v \in V_h} \frac{A_{h,\alpha}(\pi_h u - u_{h,\alpha}, v)}{|\!|\!| v |\!|\!|_{h,\alpha}} \tag{3.26}$$

$$\lesssim |\!|\!| u - \pi_h u |\!|\!|_{h,\alpha} + \sup_{v \in V_h} \frac{A_{h,\alpha}(u - u_{h,\alpha}, v)}{|\!|\!| v |\!|\!|_{h,\alpha}} \tag{3.27}$$

$$\lesssim |\!|\!| u - \pi_h u |\!|\!|_{h,\alpha} + \sup_{v \in V_h} \frac{\alpha(\nabla u, \nabla v)_{\Omega_h \setminus \Omega}}{|\!|\!| v |\!|\!|_{h,\alpha}} \tag{3.28}$$

$$\lesssim h^p \|u\|_{H^{p+1}(\Omega)} + \alpha^{1/2} h^{1/2} \|u\|_{H^2(\Omega)} \tag{3.29}$$

Here we added and subtracted an interpolant, used the identities

$$A_{h,\alpha}(u - u_{h,\alpha}, v) = A_{h,\alpha}(u, v) - L_{h,\alpha}(v) = A_{h,\alpha}(u, v) - A_{h,0}(u, v) = \alpha(\nabla u, \nabla v)_{\Omega_h \setminus \Omega} \tag{3.30}$$

and finally the estimate

$$\alpha(\nabla u, \nabla v)_{\Omega_h \setminus \Omega} \lesssim \alpha^{1/2} h^{1/2} \|u\|_{H^2(\Omega)} |\!|\!| v |\!|\!|_{h,\alpha} \tag{3.31}$$

To verify (3.31) we first note that

$$\alpha(\nabla u, \nabla v)_{\Omega_h \setminus \Omega} \lesssim \alpha \|\nabla u\|_{\Omega_h \setminus \Omega} \|\nabla v\|_{\Omega_h \setminus \Omega} \lesssim \alpha^{1/2} \|\nabla u\|_{\Omega_h \setminus \Omega} |\!|\!| v |\!|\!|_{h,\alpha} \tag{3.32}$$

By construction, and as illustrated in Fig. 3,

$$\Omega_h \setminus \Omega \subseteq U_h(\partial\Omega) \setminus \Omega = \cup_{t \in [0,h]} \partial\Omega_t \tag{3.33}$$

where $\partial\Omega_t = \{x \in U_h : \rho(x) = t\}$ and ρ is the distance function to $\partial\Omega$. Using this notation we have the estimates

$$\|\nabla u\|_{\Omega_h \setminus \Omega} \lesssim \|\nabla u\|_{U_h(\partial\Omega) \setminus \Omega} \lesssim h^{1/2} \sup_{t \in [0,h]} \|\nabla u\|_{\partial\Omega_t} \tag{3.34}$$

$$\lesssim h^{1/2} \sup_{t \in [0,h]} \|u\|_{H^2(\Omega_t)} \lesssim h^{1/2} \|u\|_{H^2(\Omega_\delta)} \lesssim h^{1/2} \|u\|_{H^2(\Omega)} \tag{3.35}$$

where we used the trace inequality $\|v\|_{\partial\Omega_t} \lesssim \|v\|_{H^1(\Omega_t)}$ with $\Omega_t = \Omega \cup (\cup_{s \in [0,t]} \partial\Omega_s)$ and $v = \nabla u$, and at last we used the stability (3.1) of the extension operator. Combining (3.32) and (3.35) we obtain (3.31). Thus the proof is complete. ■

Theorem 3.2 (L^2 *error estimate*)**.** *For $u \in H^{p+1}(\Omega)$ the following estimate holds*

$$\|u - u_{h,\alpha}\|_\Omega \lesssim h^{p+1}\|u\|_{H^{p+1}(\Omega)} + (\alpha^{1/2}h^{3/2} + \alpha h)\|u\|_{H^2(\Omega)} \tag{3.36}$$

and with α defined by (3.22) we obtain

$$\|u - u_{h,\alpha}\|_\Omega \lesssim h^{p+1}\|u\|_{H^{p+1}(\Omega)} \tag{3.37}$$

Proof. Let $\phi \in V$ be the solution to the dual problem

$$-\Delta\phi = \psi \quad \text{in } \Omega, \qquad \phi = 0 \quad \text{on } \partial\Omega \tag{3.38}$$

Posing this problem in variational form, testing with $e = u - u_{h,\alpha}$, and using that $\phi_{\partial\Omega} = 0$, gives us the identity

$$(e, \psi)_\Omega = A_{h,0}(e, \phi) - \tau h^2(\Delta e, \Delta\phi)_{\mathcal{T}_{h,\partial\Omega}\cap\Omega} \tag{3.39}$$

For the first term in (3.39) we recall that with $\alpha = 0$ we obtain a consistent method and then proceeding with the obvious estimates

$$\begin{aligned}
A_{h,0}(e, \phi) &= L_h(\phi) - A_{h,\alpha}(u_{h,\alpha}, \phi) + \alpha(\nabla u_{h,\alpha}, \nabla\phi)_{\Omega_h\setminus\Omega} && (3.40)\\
&= L_h(\phi - \pi_h\phi) - A_{h,\alpha}(u_{h,\alpha}, \phi - \pi_h\phi) + \alpha(\nabla u_{h,\alpha}, \nabla\phi)_{\Omega_h\setminus\Omega} && (3.41)\\
&= A_{h,0}(u, \phi - \pi_h\phi) - A_{h,\alpha}(u_{h,\alpha}, \phi - \pi_h\phi) + \alpha(\nabla u_{h,\alpha}, \nabla\phi)_{\Omega_h\setminus\Omega} && (3.42)\\
&= A_{h,0}(u - u_{h,\alpha}, \phi - \pi_h\phi) + \alpha(\nabla u, \nabla\pi_h\phi)_{\Omega_h\setminus\Omega} && (3.43)\\
&\lesssim |\!|\!| u - u_{h,\alpha} |\!|\!|_{h,0} |\!|\!| \phi - \pi_h\phi |\!|\!|_{h,0} + \alpha\|\nabla u\|_{\Omega_h\setminus\Omega}\|\nabla\pi_h\phi\|_{\Omega_h\setminus\Omega} && (3.44)\\
&\lesssim h|\!|\!| u - u_{h,\alpha} |\!|\!|_{h,0}\|\phi\|_{H^2(\Omega)} + \alpha h\|u\|_{H^2(\Omega)}\|\phi\|_{H^2(\Omega)} && (3.45)\\
&\le (h|\!|\!| u - u_{h,\alpha} |\!|\!|_{h,\alpha} + \alpha h\|u\|_{H^2(\Omega)})\|\psi\|_\Omega && (3.46)
\end{aligned}$$

By the dual problem and the definition of the energy norm we readily get the bound for the second term in (3.39)

$$\begin{aligned}
-\tau h^2(\Delta e, \Delta\phi)_{\mathcal{T}_{h,\partial\Omega}\cap\Omega} &\le \tau h^2\|\Delta e\|_{\mathcal{T}_{h,\partial\Omega}\cap\Omega}\|\Delta\phi\|_{\mathcal{T}_{h,\partial\Omega}\cap\Omega} && (3.47)\\
&\lesssim \tau^{1/2}h|\!|\!| u - u_{h,\alpha} |\!|\!|_{h,\alpha}\|\psi\|_\Omega && (3.48)
\end{aligned}$$

Finally, choosing $\psi = e = u - u_{h,\alpha}$ and using the energy norm estimate (3.21) we obtain

$$\|e\|_\Omega \lesssim h^{p+1}\|u\|_{H^{p+1}(\Omega)} + (\alpha^{1/2}h^{3/2} + \alpha h)\|u\|_{H^2(\Omega)} \tag{3.49}$$

which concludes the proof. ■

4. Stability of the linear system of equations

We first recall some basic concepts and then we prove an inverse estimate and a Poincaré estimate, and finally a bound on the condition number of the stiffness matrix.

4.1. Basic definitions

- The stiffness matrix $\widehat{A}$ is defined by

$$(\widehat{A}\widehat{v}, \widehat{w})_{\mathbb{R}^N} = A_{h,\alpha}(v, w) \qquad \forall v, w \in V_h \tag{4.1}$$

  where N is the dimension of V_h and $\widehat{v} \in \mathbb{R}^N$ is the coefficient vector in the expansion

$$v(x) = \sum_{i\in I} \widehat{v}_i\varphi_i(x) \tag{4.2}$$

  of v in terms of the basis functions $B = \{\varphi_i : i \in I\}$.
- The following equivalence holds

$$h^d\|\widehat{v}\|^2_{\mathbb{R}^N} \sim \|v\|^2_{\Omega_h} \qquad v \in V_h \tag{4.3}$$

- The condition number of $\widehat{A}$ is defined by

$$\kappa = \text{cond}(\widehat{A}) = \frac{\lambda_{\max}}{\lambda_{\min}} \tag{4.4}$$

where $\lambda_{\max}$ and $\lambda_{\min}$ are the largest and smallest eigenvalues of $\widehat{A}$.

We shall now derive an estimate of the condition number. In addition to the coercivity (3.15) and continuity (3.16) we will need an inverse estimate and a Poincaré estimate.

4.2. Inverse and Poincaré estimates

- The following inverse estimate holds

$$|||v|||_{h,\alpha} \lesssim h^{-1}\|v\|_{\Omega_h} \tag{4.5}$$

Proof. Recall that

$$|||v|||^2_{h,\alpha} = \|v\|^2_{a_h} + \alpha\|\nabla v\|^2_{\Omega_h\setminus\Omega} + \|v\|^2_{b_h} \tag{4.6}$$

Using standard inverse estimates

$$\begin{aligned}\|v\|^2_{a_h} + \alpha\|\nabla v\|^2_{\Omega_h\setminus\Omega} &= \|\nabla v\|^2_{\Omega} + \tau h^2\|\Delta v\|^2_{\mathcal{T}_{h,\delta}\cap\Omega} + \alpha\|\nabla v\|^2_{\Omega_h\setminus\Omega} &(4.7)\\ &\leq (1+\alpha)\|\nabla v\|^2_{\Omega_h} + \tau h^2\|\Delta v\|^2_{\Omega_h} &(4.8)\\ &\lesssim h^{-2}\|v\|^2_{\Omega_h} &(4.9)\end{aligned}$$

and using the inverse trace inequality $\|v\|^2_{\partial\Omega\cap T} \lesssim h^{-1}\|v\|^2_T$, $v \in V_h$, we get

$$\begin{aligned}\|v\|^2_{b_h} &= h^{-1}\|v\|^2_{\partial\Omega} + h\|\nabla_T v\|^2_{\partial\Omega} &(4.10)\\ &\lesssim h^{-2}\|v\|^2_{\mathcal{T}_h(\partial\Omega)} + \|\nabla v\|^2_{\mathcal{T}_h(\partial\Omega)} &(4.11)\\ &\lesssim h^{-2}\|v\|^2_{\mathcal{T}_h(\partial\Omega)} &(4.12)\\ &\lesssim h^{-2}\|v\|^2_{\Omega_h} \quad \blacksquare &(4.13)\end{aligned}$$

- The following Poincaré estimate holds

$$\alpha h^{-2}\|v\|^2_{\Omega_h\setminus\Omega} + \|v\|^2_{\Omega} \lesssim |||v|||^2_{h,\alpha} \tag{4.14}$$

and as a consequence

$$\min(1, \alpha h^{-2})\|v\|^2_{\Omega_h} \lesssim |||v|||^2_{h,\alpha} \tag{4.15}$$

Proof. Using a standard Poincaré estimate we have

$$\|v\|_{\Omega} \lesssim |||v|||_{h,0} \tag{4.16}$$

It remains to estimate $\alpha\|v\|^2_{\Omega_h\setminus\Omega}$, adding and subtracting the extension $v^e = v \circ p$, where $p : U_h \to \partial\Omega$ is the closest point mapping, and using the obvious bounds we obtain

$$\begin{aligned}\alpha\|v\|^2_{\Omega_h\setminus\Omega} &\lesssim \alpha\|v - v^e\|^2_{\Omega_h\setminus\Omega} + \alpha\|v^e\|^2_{\Omega_h\setminus\Omega} &(4.17)\\ &\lesssim \alpha h^2\|\nabla v\|^2_{\Omega_h\setminus\Omega} + \alpha\|v^e\|^2_{U_\delta\setminus\Omega} &(4.18)\\ &\lesssim \alpha h^2\|\nabla v\|^2_{\Omega_h\setminus\Omega} + \alpha h\|v\|^2_{\partial\Omega} &(4.19)\\ &\lesssim h^2\alpha\|\nabla v\|^2_{\Omega_h\setminus\Omega} + (\alpha h^2)h^{-1}\|v\|^2_{\partial\Omega} &(4.20)\\ &\lesssim h^2\max(1,\alpha)|||v|||^2_{h,\alpha} &(4.21)\end{aligned}$$

which for $\alpha < 1$ gives

$$\alpha h^{-2}\|v\|^2_{\Omega_h\setminus\Omega} \lesssim |||v|||^2_{h,\alpha} \tag{4.22}$$

Together (4.16) and (4.22) give (4.14). $\blacksquare$

4.3. Condition number estimate

Theorem 4.1 (*Condition number scaling*). *The condition number* $\kappa = \text{cond}(\widehat{A})$ *satisfies*

$$\kappa \lesssim \max(h^{-2}, \alpha^{-1}) \tag{4.23}$$

and with $\alpha \sim h^{2p-1}$,

$$\kappa \lesssim h^{-(2p-1)} \tag{4.24}$$

Proof. In view of the definition (4.4) of the condition number $\kappa = \text{cond}(\widehat{A})$ we need to estimate $\lambda_{\max}$ and $\lambda_{\min}^{-1}$.

1. To estimate $\lambda_{\max}$ we use the definition (4.1) of the stiffness matrix to pass over to the bilinear form and then we use continuity (3.16) and the equivalence (4.3) as follows

$$\lambda_{\max} = \max_{v \in V_h \setminus 0} \frac{(\widehat{A}\widehat{v}, \widehat{v})_{\mathbb{R}^N}}{\|\widehat{v}\|^2_{\mathbb{R}^N}} = \max_{v \in V_h \setminus 0} \frac{A_{h,\alpha}(v, v)}{\|\widehat{v}\|^2_{\mathbb{R}^N}} \lesssim \max_{v \in V_h \setminus 0} \frac{|||v|||^2_{h,\alpha}}{\|v\|^2_{\Omega_h}} \lesssim h^{-2} \tag{4.25}$$

2. To estimate $\lambda_{\min}^{-1}$ we again use the definition (4.1) of the stiffness matrix to pass to the bilinear form, then we use coercivity (3.15), and the equivalence (4.3),

$$\lambda_{\min}^{-1} = \max_{v \in V_h \setminus 0} \frac{\|\widehat{v}\|^2_{\mathbb{R}^N}}{(\widehat{A}\widehat{v}, \widehat{v})_{\mathbb{R}^N}} = \max_{v \in V_h \setminus 0} \frac{\|\widehat{v}\|^2_{\mathbb{R}^N}}{A_{h,\alpha}(v, v)} \lesssim \max_{v \in V_h \setminus 0} \frac{\|v\|^2_{\Omega_h}}{|||v|||^2_{h,\alpha}} \lesssim (\min(1, \alpha h^{-2}))^{-1} \tag{4.26}$$

3. Combining the estimates (4.25) and (4.26) we obtain

$$\kappa = \lambda_{\max}\lambda_{\min}^{-1} \lesssim h^{-2}(\min(1, \alpha h^{-2}))^{-1} = h^{-2}\max(1, \alpha^{-1}h^2) = \max(h^{-2}, \alpha^{-1}) \tag{4.27}$$

which completes the proof. ■

Remark 4.1 (*Finite cell stabilization trade-off*). As seen in the analysis above, the choice of how the finite cell stabilization parameter α scales with h is a trade-off between optimal order error estimates and stiffness matrix condition number scaling. This property stems from the fact that the finite cell stabilization is inconsistent (3.2), and is not specific to the least-squares stabilized Nitsche formulation. For instance, choosing $\alpha \sim h^2$ would give the standard condition number scaling of h^{-2} but would on the other hand sacrifice the optimal order of the error estimates. In this paper we instead prefer to keep the error estimates of optimal order at the cost of a suboptimal scaling of the condition number (4.24). The idea is to either remedy the condition number via preconditioning, or to use a direct solver. In the numerical results below we consider both approaches, where we utilize diagonal scaling as a simple preconditioner.

5. Numerical experiments

In this section we illustrate the stability and accuracy of the method using a 2D problem. Note however, that both the method and analysis are applicable also to problems in 3D or higher dimensions.

Implementation. The finite cell method in 2D is implemented in MATLAB and the linear system of equations is solved using a direct solver (MATLAB's \ operator). In all experiments we use tensor product quadratic B-spline basis functions, i.e. C^1-splines, on a uniform background grid. The geometry of the domain Ω is described as a high resolution polygon. When computing condition numbers the stiffness matrix $\hat{A}$ is first converted to a full matrix on which MATLAB's `eig` is applied.

Parameter choices. For the penalty parameter β we choose a fix value $\beta = 5$, since according to the analysis above this results in a method that is guaranteed coercive in any cut situation. We vary the stabilization parameter τ, which trades weight between the least-squares bulk stabilization and the effective penalization of the boundary condition in the Nitsche penalty term, see Table 1. For comparison in the results below we also include experiments using standard Nitsche boundary conditions in the finite cell method, i.e. the method (2.4) but without the new least

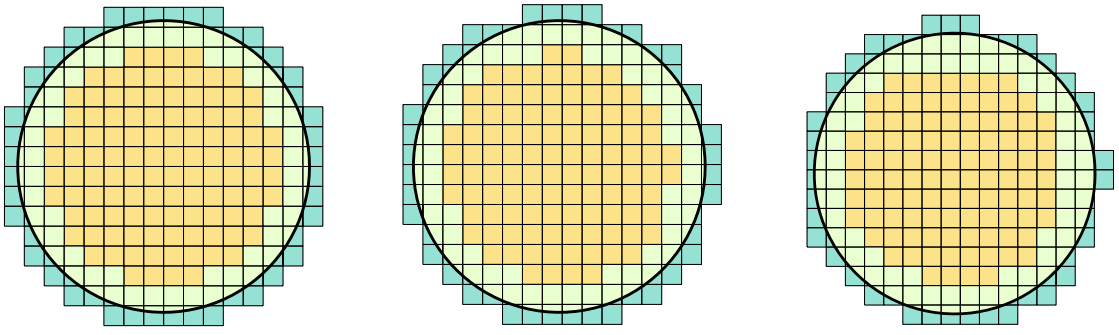

(a) $s = 0$ **(b)** $s = 0.1$ **(c)** $s = 0.2$

Fig. 4. *Shifted background grid.* Three example cut computational meshes ($h = 0.1$) for the unit disc constructed by shifting the background grid $(sh, sh/3)$ where $s \in [0, 1]$ is a parameter.

Table 1
Nitsche penalty. The effective Nitsche penalty parameter for various values of the least-squares bulk stabilization parameter τ when $\beta = 5$.

Least-squares stabilization τ	Nitsche penalty $\beta(2 + \tau^{-1})$
1	15
0.1	60
0.01	510
0.001	5010

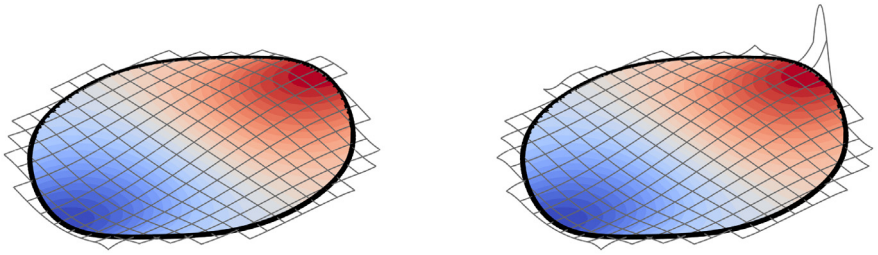

(a) LS-Nitsche **(b)** Nitsche

Fig. 5. *Solution.* Numerical solutions for the manufactured problem on the computational mesh presented in Fig. 4(c). Parameters here are $\beta = 5$ and $\tau = 0.1$ and the solution in (a) takes into account the new least-squares stabilization terms while the solution in (b) does not. The plotted solution outside the domain in (b) suggests some instabilities when not including the least-squares terms in this particular cut situation and choice of parameters.

squares stabilization terms. For a, in some sense, fair comparison, we let the effective Nitsche penalty parameter be the same so the Nitsche penalty term in both cases takes the form

$$\beta(2 + \tau^{-1})h^{-1}(v, w)_{\partial\Omega} \tag{5.1}$$

but note that we take no measures to ensure that the standard method is actually coercive.

For the finite cell stabilization in parts of the elements outside the domain, in accordance with (3.22), we set the finite cell stabilization parameter to $\alpha = 0.001h^{2p-1}$ where $p = 2$ for the quadratic B-spline basis functions. According to the analysis this should yield optimal order convergence rates of $\mathcal{O}(h^p)$ and $\mathcal{O}(h^{p+1})$ in energy respectively L^2 norms, but a suboptimal condition number scaling of $\mathcal{O}(h^{-(2p-1)})$.

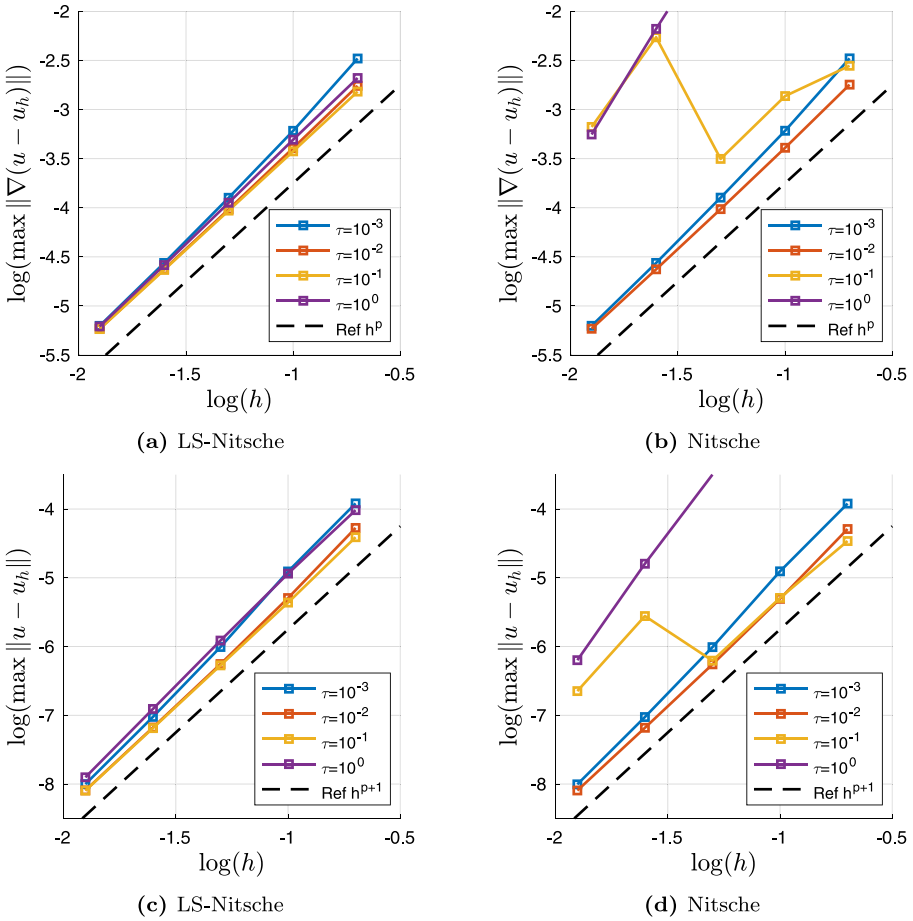

(a) LS-Nitsche **(b)** Nitsche

(c) LS-Nitsche **(d)** Nitsche

Fig. 6. *Convergence.* Worst case convergence for a finite cell method with least squares stabilized Nitsche boundary conditions respectively standard Nitsche boundary conditions, both with the same effective penalty parameter.

Experiments. We manufacture a problem with known analytical solution on the unit disc $\Omega = \{(x, y) : x^2+y^2 < 1\}$ via the ansatz

$$u(x, y) = \frac{1}{10}\left(\sin(2x) + x\cos(3y)\right) \tag{5.2}$$

from which we derive data $f : \Omega \to \mathbb{R}$ and $g : \partial\Omega \to \mathbb{R}$. To increase the probability of encountering problematic cut situations, for a given mesh size we perform computations on meshes extracted from 100 different shifts of the background grid and select the worst case. Specifically, the background grid is shifted $(sh, sh/3)$ where $s \in [0, 1]$ is a parameter that we vary from 0 to 1 in 100 increments. Three example meshes are presented in Fig. 4. Finite cell solutions to the manufactured problem in one cut situation are presented in Fig. 5 with least-squares Nitsche stabilized boundary conditions respectively standard Nitsche boundary conditions. In this example we note an additional smoothness of the solution when we include the least-squares terms.

Convergence. To illustrate the optimal order error estimates (3.23) and (3.37) in Fig. 6 we present convergence results in H^1 seminorm and in L^2 norm for the manufactured problem using various values of τ for the finite cell method with least-squares stabilized Nitsche boundary conditions respectively standard Nitsche boundary conditions. For each mesh size h the largest error among the 100 different cut situations is presented, yielding a sort of worst case convergence. When using least-squares stabilized Nitsche boundary conditions the finite cell method achieves

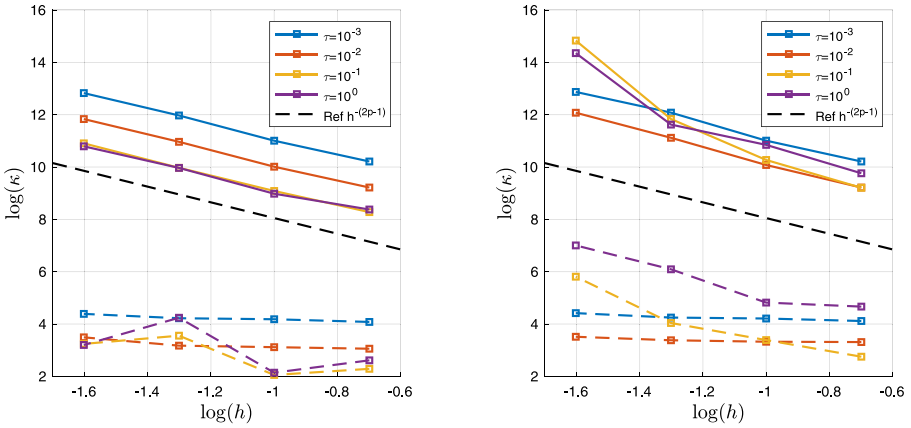

(a) LS-Nitsche **(b)** Nitsche

Fig. 7. *Condition number scaling.* Worst case scaling of the condition number for a finite cell method with least squares stabilized Nitsche boundary conditions respectively standard Nitsche boundary conditions, both with the same effective penalty parameter. The dashed lines are the corresponding condition numbers after preconditioning using diagonal scaling.

optimal order convergence for all values of τ, while the method with standard Nitsche boundary conditions fails in this task for the larger values $\tau = 1$ and $\tau = 0.1$. The reason is most likely that the standard Nitsche method is then non-coercive in the worst cut situations. For lower values of τ, which means a larger effective Nitsche penalty, we do not see this failure when using standard Nitsche boundary conditions. We do, however, see an increasing magnitude for the errors as τ is lowered which we attribute to locking due to the geometry being curved inside elements in combination with an increasing magnitude of the effective Nitsche penalty. Overall we achieve the best performance in this experiment using $\tau = 0.1$ and least-squares stabilized Nitsche boundary conditions.

Condition number. To illustrate the condition number scaling (4.24) we, analogously to the convergence experiment, present worst case scalings for the stiffness matrix condition number in Fig. 7. In accordance with theory the finite cell method with least-square stabilized Nitsche boundary conditions produce condition numbers that scales as $\mathcal{O}(h^{-(2p-1)})$, while the method with standard Nitsche boundary conditions fails to achieve this bound when τ is large ($\tau = 1, \tau = 0.1$). As in the case of the worst case convergence we suspect that the standard method is non-coercive in those situations. While we do not see such failures in the standard method when using smaller values of τ, we note that choosing a smaller τ seems to have a significant effect of increasing the magnitude of the condition numbers. We also note that diagonal scaling seems to work very well as a preconditioner for the method.

In Fig. 8 we get a view of how the condition numbers vary over 500 different cut situations for the disc on a fixed mesh size, and we see the least-squares stabilization seems to have a very positive effect for larger values of τ. Again, we see the effectiveness of diagonal scaling. In particular, the combination of finite cell stabilization, LS-Nitsche and diagonal scaling seems confidence inspiring. However, in (d)–(f) at around $s = 0.35$, we see some minor disturbance and discontinuity, which could warrant further investigation, but we believe this is likely caused by extreme cut situations.

Finally, in Fig. 9 we investigate the condition number in two special cases. Both cases are constructed such that the elements with the smallest intersection with the domain is $\sim \delta^2$ of a full element, and the parameter $\delta > 0$ is varied. Further details of the two cases are given in the caption. In these experiments we also consider different values for the finite cell stabilization parameter, including zero, as well as preconditioning by diagonal scaling. For the first special case, Figs. 9(a)–9(c), it becomes apparent that without finite cell stabilization, the condition number can become arbitrarily high, and this is not solved by the preconditioning. Including only a small amount of finite cell stabilization seems sufficient to bound the condition number. In the second special case, Figs. 9(d)–9(f), the condition number of the system seems bounded even without finite cell stabilization. The effect of the least-squares stabilization terms does not seem to be essential in these experiments, but they generally give some improvement. Diagonal scaling on the other hand seems to work well as long as some finite cell stabilization is included.

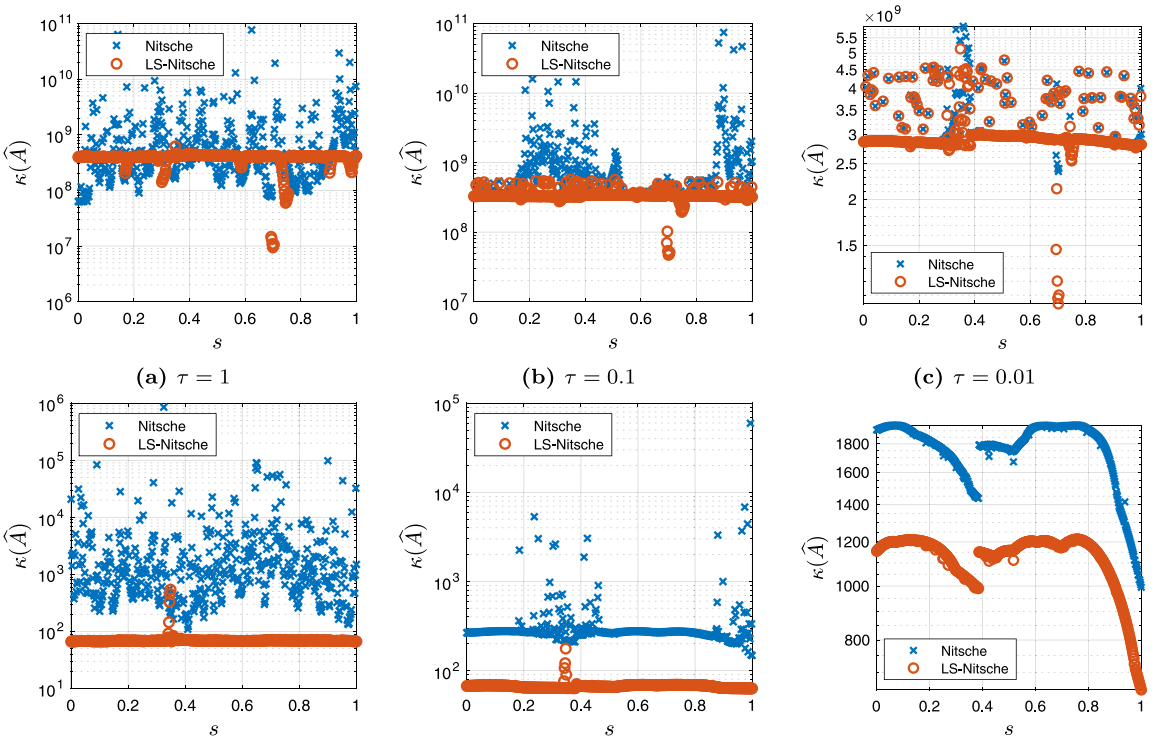

(a) $\tau = 1$ (b) $\tau = 0.1$ (c) $\tau = 0.01$

(d) $\tau = 1$, preconditioned (e) $\tau = 0.1$, preconditioned (f) $\tau = 0.01$, preconditioned

Fig. 8. *Condition number variation.* Condition numbers for the stiffness matrices on the unit disc assembled using 500 different shifts of the background grid ($h = 0.13$).

6. Conclusions

In this contribution we have used a least-squares stabilized Nitsche formulation to enforce Dirichlet boundary conditions in the finite cell method with C^1 splines. Our analysis and numerical experiments show the following:

- The method is symmetric and features guaranteed coercivity in every cut situation, a property that does not depend on choosing a large penalty parameter. Since both the finite cell stabilization and the least-squares Nitsche stabilization terms are added element-wise, implementation in element based codes is straightforward.
- In numerical experiments the method exhibits remarkable stability, both regarding convergence and conditioning, even in extreme cut situations using a moderate effective Nitsche penalty parameter (~ 10).
- The finite cell stabilization guarantees a symmetric positive definite stiffness matrix, but due to inconsistency (3.2) it gives a suboptimal h-scaling of the condition number when tuned for optimal order error estimates ($\alpha \sim h^{2p-1}$). We therefore suggest to combine the method with a suitable preconditioner or to use a direct solver.
- Diagonal scaling seems to work quite well as a preconditioner for the method. While during our numerical experiments we have not seen a case where it breaks down when both the least-squares Nitsche stabilization terms and finite cell stabilization are included, we assume the method is not immune to the effect of cut basis functions being almost linearly dependent, in particular for higher order basis functions, see [19,20].

Overall, this combination of techniques for enforcing Dirichlet conditions in unfitted FEMs seems very promising.

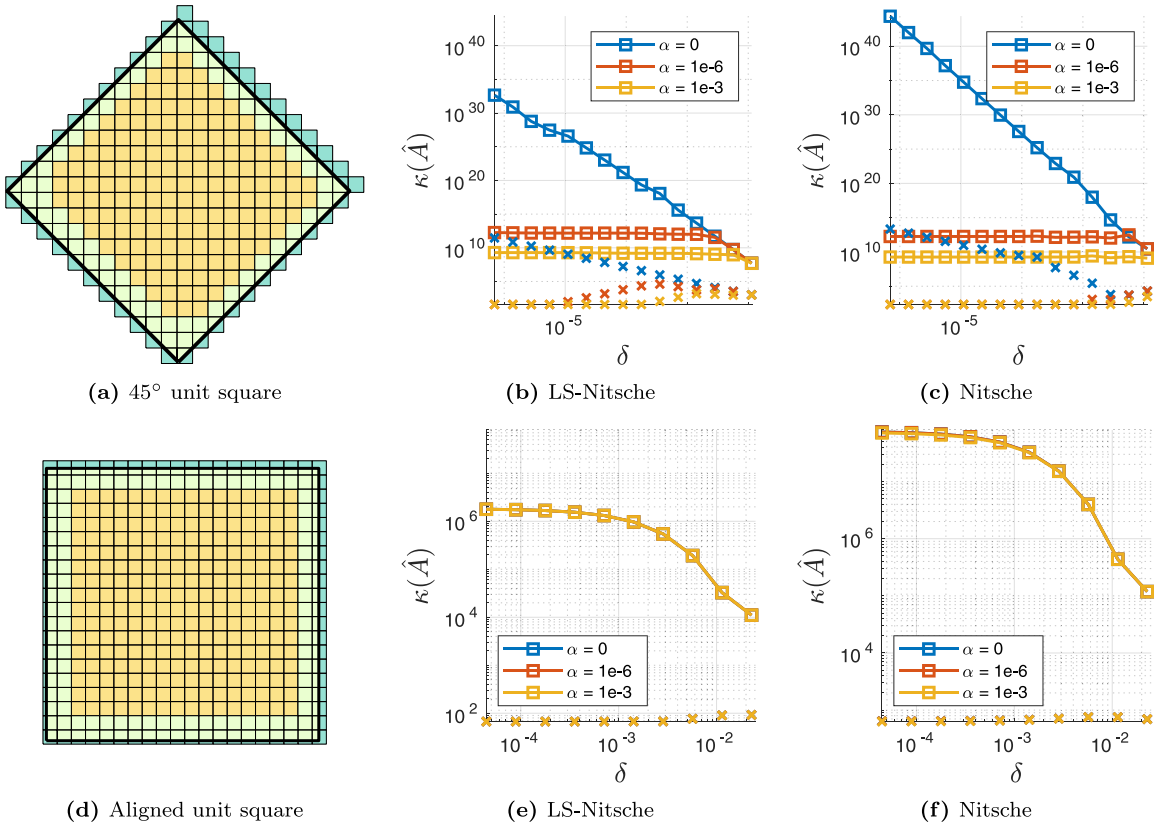

(a) 45° unit square (b) LS-Nitsche (c) Nitsche

(d) Aligned unit square (e) LS-Nitsche (f) Nitsche

Fig. 9. *Condition numbers in two special cases.* Here two cases have been artificially constructed such that we create in a controlled way elements with an arbitrary small intersection with the domain depending on a parameter $\delta > 0$, where smaller δ means a smaller intersection. The finite cell stabilization is here varied to show its effect on the condition numbers. Note that to the values $\alpha = \{0, \text{1e-6}, \text{1e-3}\}$ stated in the legends of these plots, the scaling h^{2p-1} is also applied, and hence these values correspond to effective finite cell parameters of roughly $\alpha = \{0, 10^{-10}, 10^{-7}\}$ in both cases. *First case:* The geometry and mesh ($h = 0.09$) are illustrated in (a), where the background grid is placed so that all cut elements are precisely half elements, after which the geometry is shifted diagonally $(\delta h, \delta h)/\sqrt{2}$ creating arbitrarily small cut elements on the upper right side whose area is $\sim \delta^2$ of a full element. The condition numbers for this case are presented in (b) and (c), where crosses denote condition numbers after diagonal scaling. *Second case:* The geometry and mesh ($h = 0.07$) are illustrated in (d), where the background grid is placed perfectly matching the geometry, after which the geometry is shifted diagonally (δ, δ) creating arbitrarily small cut elements on the right and upper sides whose area is $\sim \delta$ of a full element and a corner element whose area is $\sim \delta^2$ of a full element. The condition numbers for this case are presented in (e) and (f), where crosses denote the corresponding condition numbers after diagonal scaling.

Declaration of competing interest

The authors declare that they have no known competing financial interests or personal relationships that could have appeared to influence the work reported in this paper.

Acknowledgments

The first and last authors greatly acknowledge the funds provided by the Swedish Foundation for Strategic Research Grant No. AM13-0029, the Swedish Research Council Grants Nos. 2017–03911, 2021–04925, and the Swedish Research Programme Essence. The second and third authors greatly acknowledge the funds provided by the Deutsche Forschungsgemeinschaft (DFG – German Research Foundation) Grants KO 4570/1-1 and RA 627/29-1.

References

[1] J. Parvizian, A. Düster, E. Rank, Finite cell method: h- and p-extension for embedded domain problems in solid mechanics, Comput. Mech. 41 (1) (2007) 121–133, http://dx.doi.org/10.1007/s00466-007-0173-y.

[2] A. Hansbo, P. Hansbo, An unfitted finite element method, based on nitsche's method, for elliptic interface problems, Comput. Methods Appl. Mech. Engrg. 191 (47–48) (2002) 5537–5552, http://dx.doi.org/10.1016/S0045-7825(02)00524-8.
[3] E. Burman, S. Claus, P. Hansbo, M.G. Larson, A. Massing, CutFEM: discretizing geometry and partial differential equations, Internat. J. Numer. Methods Engrg. 104 (7) (2015) 472–501, http://dx.doi.org/10.1002/nme.4823.
[4] J. Haslinger, Y. Renard, A new fictitious domain approach inspired by the extended finite element method, SIAM J. Numer. Anal. 47 (2) (2009) 1474–1499, http://dx.doi.org/10.1137/070704435.
[5] A. Düster, J. Parvizian, Z. Yang, E. Rank, The finite cell method for three-dimensional problems of solid mechanics, Comput. Methods Appl. Mech. Engrg. 197 (45–48) (2008) 3768–3782, http://dx.doi.org/10.1016/j.cma.2008.02.036.
[6] J. Nitsche, Über ein variationsprinzip zur lösung von Dirichlet-problemen bei verwendung von teilräumen, die keinen randbedingungen unterworfen sind, Abh. Math. Semin. Univ. Hambg. 36 (1971) 9–15, http://dx.doi.org/10.1007/BF02995904.
[7] E. Burman, Ghost penalty, C. R. Math. Acad. Sci. Paris 348 (21–22) (2010) 1217–1220, http://dx.doi.org/10.1016/j.crma.2010.10.006.
[8] A. Johansson, M.G. Larson, A high order discontinuous Galerkin Nitsche method for elliptic problems with fictitious boundary, Numer. Math. 123 (4) (2013) 607–628, http://dx.doi.org/10.1007/s00211-012-0497-1.
[9] D. Elfverson, M.G. Larson, K. Larsson, CutIGA with basis function removal, Adv. Model. Simul. Eng. Sci. 5 (6) (2018) 1–19, http://dx.doi.org/10.1186/s40323-018-0099-2.
[10] M. Dauge, A. Düster, E. Rank, Theoretical and numerical investigation of the finite cell method, J. Sci. Comput. 65 (3) (2015) 1039–1064, http://dx.doi.org/10.1007/s10915-015-9997-3.
[11] S. Kollmannsberger, A. Özcan, J. Baiges, M. Ruess, E. Rank, A. Reali. Parameter-free, Weak imposition of Dirichlet boundary conditions and coupling of trimmed and non-conforming patches, Internat. J. Numer. Methods Engrg. 101 (9) (2015) 670–699, http://dx.doi.org/10.1002/nme.4817.
[12] D. Schillinger, A. Düster, E. Rank, The *hp-d*-adaptive finite cell method for geometrically nonlinear problems of solid mechanics, Internat. J. Numer. Methods Engrg. 89 (9) (2012) 1171–1202, http://dx.doi.org/10.1002/nme.3289.
[13] D. Schillinger, M. Ruess, The finite cell method: a review in the context of higher-order structural analysis of CAD and image-based geometric models, Arch. Comput. Methods Eng. 22 (3) (2015) 391–455, http://dx.doi.org/10.1007/s11831-014-9115-y.
[14] B. Wassermann, S. Kollmannsberger, S. Yin, L. Kudela, E. Rank, Integrating CAD and numerical analysis: 'dirty geometry' handling using the finite cell method, Comput. Methods Appl. Mech. Engrg. 351 (2019) 808–835, http://dx.doi.org/10.1016/j.cma.2019.04.017.
[15] D. Kamensky, M.-C. Hsu, D. Schillinger, J.A. Evans, A. Aggarwal, Y. Bazilevs, M.S. Sacks, T.J.R. Hughes, An immersogeometric variational framework for fluid–structure interaction: application to bioprosthetic heart valves, Comput. Methods Appl. Mech. Engrg. 284 (2015) 1005–1053, http://dx.doi.org/10.1016/j.cma.2014.10.040.
[16] D. Elfverson, M.G. Larson, K. Larsson, A new least squares stabilized nitsche method for cut isogeometric analysis, Comput. Methods Appl. Mech. Engrg. 349 (2019) 1–16, http://dx.doi.org/10.1016/j.cma.2019.02.011.
[17] G.B. Folland, Introduction to Partial Differential Equations, second ed., Princeton University Press, Princeton, 1995.
[18] L. Beirão da Veiga, A. Buffa, G. Sangalli, R. Vázquez, Mathematical analysis of variational isogeometric methods, Acta Numer. 23 (2014) 157–287, http://dx.doi.org/10.1017/S096249291400004X.
[19] F. de Prenter, C.V. Verhoosel, G.J. van Zwieten, E.H. van Brummelen, Condition number analysis and preconditioning of the finite cell method, Comput. Methods Appl. Mech. Engrg. 316 (2017) 297–327, http://dx.doi.org/10.1016/j.cma.2016.07.006.
[20] F. de Prenter, Preconditioned Iterative Solution Techniques for Immersed Finite Element Methods: With Applications in Immersed Isogeometric Analysis for Solid and Fluid Mechanics, (Ph.D. thesis), Technische Universiteit Eindhoven, 2019.